Human Molecular Genetics, 2007, Vol. 16, No. 19 **2359–2365**
doi:10.1093/hmg/ddm193
Advance Access published on July 17, 2007

Overexpression of mutant superoxide dismutase 1 causes a motor axonopathy in the zebrafish

Robin Lemmens[1,2,*†], Annelies Van Hoecke[1,†], Nicole Hersmus[1], Veerle Geelen[1], Isabel D'Hollander[2], Vincent Thijs[2], Ludo Van Den Bosch[1], Peter Carmeliet[3,4] and Wim Robberecht[1,2]

[1]Laboratory of Neurobiology and [2]Department of Neurology, University Hospital Gasthuisberg, K.U. Leuven, Herestraat 49, B-3000 Leuven, Belgium, [3]Department for Transgene Technology and Gene Therapy, VIB, 3000 Leuven, Belgium and [4]The Centre for Transgene Technology and Gene Therapy (CTG), K.U. Leuven, B-3000 Leuven, Belgium

Received May 25, 2007; Revised and Accepted July 14, 2007

The development of small animal models is of major interest to unravel the pathogenesis and treatment of neurodegenerative diseases, especially because of their potential in large-scale chemical and genetic screening. We have investigated the zebrafish as a model to study amyotrophic lateral sclerosis (ALS), a fatal neurodegenerative disorder characterized by the selective loss of motor neurons, caused by mutations in superoxide dismutase 1 (SOD1) in a subset of patients. Overexpression of mutant human SOD1 in zebrafish embryos induced a motor axonopathy that was specific, dose-dependent and found for all mutations studied. Moreover, using this newly established animal model for ALS, we investigated the role of a known modifier in the disease: vascular endothelial growth factor (VEGF). Lowering VEGF induced a more severe phenotype, whereas upregulating VEGF rescued the mutant SOD1 axonopathy. This novel zebrafish model underscores the potential of VEGF for the treatment of ALS and furthermore will permit large-scale genetic and chemical screening to facilitate the identification of new therapeutic targets in motor neuron disease.

INTRODUCTION

Neurodegenerative diseases are a major medical and socio-economic problem in western countries. Developing a therapeutic strategy for these disorders requires the identification of the genetic and pathogenic factors involved. Small animal models such as flies and worms have been shown to be useful tools to unravel the mechanism of neurodegeneration and have been generated for some, such as Huntington's disease and other inherited polyglutamine disorders (1). The potential of the zebrafish for research in neurodegeneration has been investigated to a limited extent so far. We have explored a zebrafish model for amyotrophic lateral sclerosis (ALS). ALS is a neurodegenerative disease characterized by the selective loss of motor neurons in the spinal cord, brainstem and motor cortex, which gives rise to muscle weakness and atrophy. The disease is uniformly fatal, usually after a relentlessly progressive course of 3–5 years. Most ALS patients have the sporadic form of the disease (SALS), whereas 10% has a familial, usually autosomal dominant form (FALS). In one out of five of such families, mutations in the superoxide dismutase 1 (SOD1) gene underlie the disease (2). SALS is thought to arise from an interaction between genetic risk factors, aging of the nervous system and possibly also environmental factors. Disease-modifying genes are also involved in the pathogenesis of mutant SOD1-associated ALS, given the vast variability in disease expression in patients carrying the same mutation (3).

Currently, there is no cure for ALS. Screens of libraries of small compounds with potential therapeutic effect, and genetic screens aimed to identify modifying pathways and new pharmacological targets, are hampered by the lack of a

*To whom correspondence should be addressed at: Laboratory of Neurobiology and Department of Neurology, University Hospital Gasthuisberg, K.U. Leuven, Herestraat 49, B-3000 Leuven, Belgium. Tel: +32 16344280; Fax: +32 16344285; Email: robin.lemmens@med.kuleuven.be
†The authors wish it to be known that, in their opinion, the first two authors should be regarded as joint First Authors.

small animal model. Such studies in the available mouse and rat models are time-consuming and very costly, and attempts to model mutant SOD1-associated ALS in *Caenorhabditis elegans* and *Drosophila* have not been successful so far (4,5). In addition, many screens have concentrated on survival of the motor neuron perikaryon, rather than on the integrity of the axon, at the risk of identifying compounds that rescue the neuron but not the organism (6).

We have explored the potential of the zebrafish as a model for a neurodegenerative disease. This organism is becoming a promising tool for drug discovery (7,8). A zebrafish model for a dominant, gain-of-function caused neurodegenerative disease has not been reported hitherto. Nevertheless, a major advantage of the zebrafish model is that spinal motor axons are easily identifiable in the zebrafish embryo and have been extensively described in both normal and pathological conditions (9,10), which makes it an attractive model to study diseases such as ALS. Motor axonal dysfunction, indeed, is the first manifestation of ALS in both human patients and mutant SOD1-overexpressing mice, a reliable rodent model for ALS (11). Motor axonal abnormalities in the mouse model are known to occur as early as the first post-natal week in $SOD1^{G85R}$ mice (12).

We here describe modeling of mutant SOD1-associated ALS in the zebrafish embryo and the effect of vascular endothelial growth factor (VEGF) and wild type SODI ($SOD1^{WT}$) on the identified motor axonopathy.

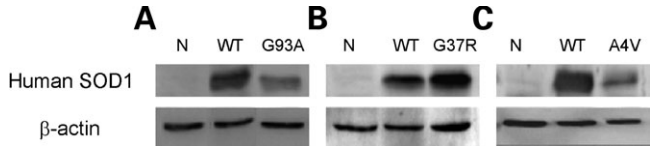

Figure 1. Overexpression of human SOD1 after mRNA injection. Expression of $SOD1^{WT}$, $SOD1^{G93A}$, $SOD1^{G37R}$ and $SOD1^{A4V}$ in zebrafish embryos 30 hpf. In each first lane, normal (uninjected) embryos (N) were loaded, $SOD1^{WT}$-injected embryos are shown in each second lane (WT) and the third lane contains protein extracts from mutant SOD1-injected embryos. (**A**) $SOD1^{G93A}$; (**B**) $SOD1^{G37R}$ and (**C**) $SOD1^{A4V}$. β-Actin was used as a loading control.

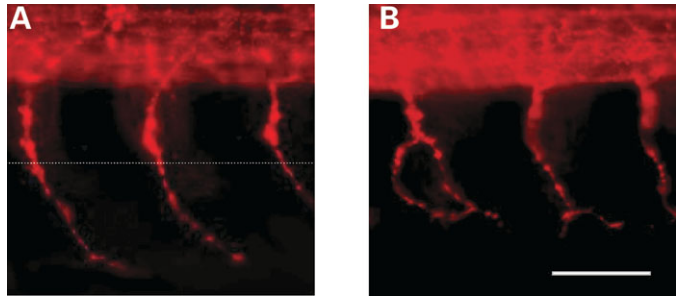

Figure 2. Specific motor axonal defects in embryos injected with mutant SOD1 mRNA. Injection with $SOD1^{A4V}$ 1500 ng/μl induced branching in primary motor neurons (**B**), compared with $SOD1^{WT}$ (**A**). White dashed line defines the ventral edge of the notochord. Scale bar: 50 μm.

RESULTS

Expression of *SOD1* protein

We injected mRNA encoding human $SOD1^{WT}$ and three different mutant SOD1 ($SOD1^{MT}$): $SOD1^{G93A}$, $SOD1^{G37R}$ and $SOD1^{A4V}$ in a concentration of 1000 ng/μl. The level of expression of these proteins at 30 h post-fertilization (hpf) was determined using western blotting (Fig. 1). $SOD1^{WT}$ was expressed somewhat more abundantly than $SOD1^{G93A}$ and $SOD1^{A4V}$ and appeared to be more stable than $SOD1^{MT}$, as has been reported before (13).

Mutant *SOD1* induces a motor axonopathy

Following mRNA-injection, only embryos with normal morphology and development were used for further analysis (more than 85% of the embryos injected). Abnormal branching and length of motor neuron axons were measured in both $SOD1^{MT}$ and $SOD1^{WT}$ overexpressing fish at 30 hpf. Motor neurons were scored as abnormal when axons branched at or above the ventral edge of the notochord (Fig. 2). Embryos were scored affected when two or more axons per embryo showed aberrant branching. Overexpression of $SOD1^{WT}$ (1000 ng/μl) had no effect on axonal outgrowth of motor neurons when compared with buffer-injected control embryos. In contrast, overexpression of $SOD1^{A4V}$, $SOD1^{G93A}$ and $SOD1^{G37R}$ (1000 ng/μl) induced clear motor axonal abnormalities. Expression of $SOD1^{G93A}$ or $SOD1^{G37R}$ caused 64.6 and 68.8% of the embryos to be affected respectively, with 12.4 and 12.5% of axons showing abnormal branching per embryo on average, respectively (Table 1). The most pronounced effect was seen when embryos expressed $SOD1^{A4V}$, with 73.1% of the embryos being affected with an average of 13.1% aberrant axons per embryo. The average axonal length of 10 ventral motor axons per embryo was determined and was significantly decreased by 6.1% of normal length after $SOD1^{G93A}$ expression, by 14.5% after $SOD1^{G37R}$ expression and by 18.0% after $SOD1^{A4V}$ expression (Fig. 3A).

As $SOD1^{A4V}$ resulted in the most striking phenotype, a dose–response test was performed using this mutation. As the statistical analysis was identical if the length of only five axons per embryo was evaluated, we limited measurements to the five most proximal axons. Embryos were injected with four doses 250, 500, 1000 and 1500 ng/μl $SOD1^{A4V}$ mRNA and axonal defects were compared with embryos injected with 1500 ng/μl $SOD1^{WT}$ mRNA. We found 16.1, 34.4, 68.4 and 80.6% of the embryos to be affected, respectively, and thus this effect to be dose responsive. The percentage of anomalous axons per embryo equally showed a dose relation with 16.9% of axons showing abnormalities at the highest dose used (Table 2). A similar dose–response relationship was found for axonal length (Pearson's correlation: -0.73, $P < 0.001$), with a decrease of 23% at a dose of 1500 ng/μl $SOD1^{A4V}$ mRNA (Fig. 3B).

When morphologically normal embryos at 30 hpf were followed during 7 days post-fertilization, we did not observe a significant difference in survival between $SOD1^{WT}$ and $SOD1^{A4V}$ (1500 ng/μl) injected embryos.

Effect of mutant *SOD1* is specific for motor axons

Although we only evaluated embryos with a normal morphology, we wanted to exclude subtle developmental delay

Table 1. Mutant SOD1 induces abnormal branching

	Affected embryos (%)	Odds ratio (CI)	*P*-value	Branching axons per embryo (%)	*P*-value (Mann–Whitney test)
WT, $n = 101$	27.7			4.8	
G93A, $n = 48$	64.6	4.8 (2.3–9.9)	1.7×10^{-5}	12.4	1.0×10^{-5}
G37R, $n = 32$	68.8	5.7 (2.4–13.6)	3.0×10^{-5}	12.5	2.1×10^{-6}
A4V, $n = 52$	73.1	7.1 (3.3–15.0)	8.1×10^{-8}	13.1	3.3×10^{-10}

After injection with three different SOD1 mutants (concentration: 1000 ng/μl), we observed abnormal branching of caudal primary motor neurons when compared with $SOD1^{WT}$ (concentration: 1000 ng/μl). This effect was most pronounced when using the A4V-mutant. $SOD1^{WT}$ did not induce abnormalities of axonal outgrowth.

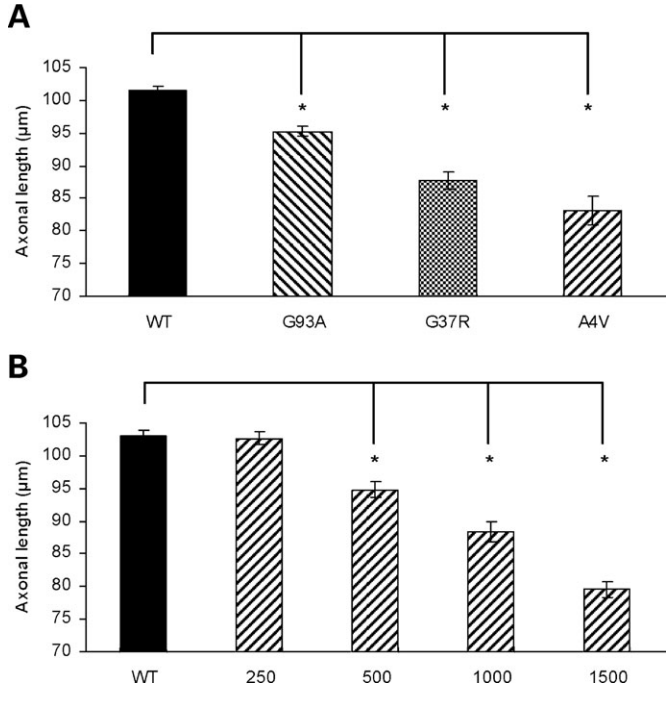

Figure 3. Different SOD1 mutants induce shortening of motor neuron axons. Mutant SOD1 induces shortening of primary motor neurons after injection with three different mutants G93A ($n = 48$), G37R ($n = 32$) and A4V ($n = 52$), compared with $SOD1^{WT}$ ($n = 101$) when injected at the same concentration (1000 ng/μl) (**A**). This effect is shown to be dose-dependent when $SOD1^{A4V}$ is injected at various concentrations and compared with $SOD1^{WT}$ injected at the highest dose used (1500 ng/μl) (**B**). WT 1500 ng/μl $n = 30$, A4V 250 ng/μl $n = 31$, A4V 500 ng/μl $n = 32$, A4V 1000 ng/μl $n = 38$, A4V 1500 ng/μl $n = 31$. *Y*-error bars represent standard error of the mean. $^*P < 0.001$.

by measuring the total length of the different embryos. This parameter was found not to be different between $SOD1^{WT}$ and $SOD1^{MT}$ mRNA-injected embryos.

To determine whether the motor axon abnormalities were specific, we investigated various other axonal systems at 30 hpf. First, we studied the commissural axon of the Mauthner neuron in the hindbrain. No differences in the projection of these axons across the midline and down the spinal cord between $SOD1^{WT}$ and $SOD1^{MT}$ overexpressing embryos were observed (data not shown). Similarly, the morphology of the lateral line, a group of sensory neurons that sends axons over the entire length of the zebrafish embryo, and Rohon–Beard sensory neurons did not show major defects after injection with $SOD1^{MT}$ (Supplementary Material, Fig. S1A–D), whereas expression of $SOD1^{MT}$ in these axons was similar to that in motor axons, as estimated immunohistochemically (Supplementary Material, Fig. S2).

Validation of the zebrafish model

In order to provide evidence that the model described can be used as a chemical and/or genetic screening tool, we investigated whether the abnormalities induced by $SOD1^{MT}$ could be affected by two factors known to modify (rescue or aggravate) the phenotype of mutant SOD1-associated motor neuron degeneration in rodent models, VEGF and $SOD1^{WT}$ (14–18).

Axonal defects of motor neurons are rescued by VEGF. Increasing VEGF availability to motor neurons is of benefit to rodents with mutant SOD1-induced motor neuron degeneration (14,17). To investigate the effect of VEGF on the axonopathy induced by $SOD1^{MT}$, we treated zebrafish embryos with GS4012, which has been shown to upregulate VEGF in zebrafish embryos (8). We confirmed the upregulation of VEGF by real-time polymerase chain reaction (PCR) and found an increase of 18% after treatment with 1 ng/μl GS4012 (data not shown). At this dose, the effect on axonal length in $SOD1^{A4V}$ was completely rescued. The decrease in axonal length induced by $SOD1^{A4V}$ when compared with $SOD1^{WT}$ observed in controls ($n = 31$) was 18.5% versus a 2.1% increase in VEGF-inducer treated embryos ($n = 32$, $P < 0.001$). The substance did not induce an increase in axonal length in $SOD1^{WT}$-injected embryos, excluding a general neurotrophic effect. GS4012 increased the percentage of affected embryos injected with $SOD1^{WT}$ from 20.7 to 34.5%, showing the inherent effect of the compound. After correction for this relative increase, GS4012 significantly rescued the $SOD1^{A4V}$-induced branching abnormalities: 35.6% of affected embryos in the GS4012-treated group versus 70.0% of affected embryos in the vehicle-treated group ($P = 0.0068$).

Lowering VEGF induces a more severe effect on axonal outgrowth. Low VEGF expression is a risk factor for motor neuron degeneration in both animals and humans (15,16). The effect of knockdown of VEGF using morpholinos (MO) has been investigated in vascular development of zebrafish embryos (19). MO knockdown is an antisense technology used to sterically block access of other molecules to RNA; an ATG MO obstructs the forming of the initiation complex

Table 2. Injection with $SOD1^{A4V}$ results in dose-dependent abnormal branching

	Affected embryos (%)	Odds ratio (CI)	*P*-value	Branching axons per embryo (%)
WT 1500 ng/μl, $n = 30$	13.3[a]			4.0[b]
A4V 250 ng/μl, $n = 31$	16.1[a]	1.3 (0.3–5.2)	0.76	3.1[b]
A4V 500 ng/μl, $n = 32$	34.4[a]	3.4 (0.9–12.3)	0.053	6.6[b]
A4V 1000 ng/μl, $n = 38$	68.4[a]	14.1 (4.0–49.4)	5.6×10^{-6}	10.5[b]
A4V 1500 ng/μl, $n = 31$	80.6[a]	27.1 (6.8–107.6)	1.4×10^{-7}	16.9[b]

After injection with $SOD1^{A4V}$, primary motor neurons showed anomalous branching in a dose-dependent manner when compared with $SOD1^{WT}$ overexpressing embryos, which were injected at the highest concentration used (1500 ng/μl).
[a]Spearman's correlation: 0.55, *P*-value: 1.0×10^{-6}; Kruskal–Wallis *P*-value: 3.8×10^{-13}.
[b]Spearman's correlation: 0.58, *P*-value: 1.0×10^{-6}; Kruskal–Wallis *P*-value: 6.6×10^{-15}.

Table 3. Lowering VEGF exacerbates the mutant SOD1 phenotype

	Affected embryos (%)	Odds ratio (CI)	*P*-value	Branching axons per embryo (%)
WT 500 ng/μl + 3 ng Ctr-MO, $n = 32$	9.4			3.3
A4V 500 ng/μl + 3 ng Ctr-MO, $n = 35$	28.6			5.7
A4V 500 ng/μl + 3 ng VEGF-MO, $n = 36$	52.8	2.8 (1.0–7.5)	0.038	8.6[a]

Co-injection of VEGF-MO and $SOD1^{A4V}$ induced abnormal branching in significantly more embryos when compared with Ctr-MO and $SOD1^{A4V}$-injected embryos.
[a]$SOD1^{A4V}$ + Ctr-MO versus $SOD1^{A4V}$ + VEGF-MO, $P = 0.027$.

during the first step of transcription. We co-injected the published VEGF-ATG-MO (3 ng) (19) with $SOD1^{A4V}$ mRNA (500 ng/μl) in zebrafish embroys and compared the effect on axonal abnormalities to embroys co-injected with a standard control MO (3 ng) and $SOD1^{A4V}$ mRNA. Knockdown of VEGF was confirmed, as we observed the severe effect on blood vessel formation by the VEGF-MO in these embryos consistent with previous reports (19,20). Lowering VEGF increased the number of embryos with abnormal axonal branching induced by $SOD1^{A4V}$ with 24.2%, as well as the number of abnormally branching axons per embryo (Table 3). Decreasing VEGF levels also further reduced axonal length in $SOD1^{A4V}$ overexpressing embryos (Fig. 4A). Hence, the motor axonopathy in zebrafish induced by mutant SOD1 was aggravated by lowering VEGF expression, consistent with findings in animal models of ALS (15).

Co-expression of WT aggravates the mutant phenotype. As $SOD1^{WT}$ has been reported not to influence $SOD1^{MT}$-induced motor neuron degeneration in mice (21), although recently was shown to be able to convert an unaffected phenotype to an ALS phenotype in the mutant $SOD1^{A4V}$ transgenic mouse (18), we investigated the effect of $SOD1^{WT}$ in the zebrafish model. $SOD1^{WT}$ and $SOD1^{A4V}$ mRNA were co-injected at the same doses (500 ng/μl) and axonal outgrowth was compared with that seen after injection of $SOD1^{A4V}$ mRNA (500 ng/μl), whereas $SOD1^{WT}$ mRNA (1000 ng/μl) was used as the first control (same amount of mRNA as in the co-injection) and co-injection of green fluorescent protein (GFP) mRNA (500 ng/μl) with $SOD1^{A4V}$ mRNA (500 ng/μl) was utilized as a second control condition. Overexpression of $SOD1^{WT}$ increased the number of affected embryos with 30.4% and significantly increased the percentage of abnormally branching axons per embryo (Table 4). Similarly, $SOD1^{WT}$ overexpression aggravated the effect of $SOD1^{A4V}$ on axonal length (Fig. 4B). In contrast, co-expression of GFP and $SOD1^{A4V}$ did not affect the phenotype. Quantitatively, the co-injection of 500 ng/μl of $SOD1^{WT}$ mRNA and 500 ng/μl of $SOD1^{A4V}$ mRNA affected axonal outgrowth to the same extent as did 1000 ng/μl of $SOD1^{A4V}$ mRNA (Table 4).

DISCUSSION

Our findings demonstrate that overexpression of $SOD1^{MT}$ induces a very robust and easily to monitor axonopathy in the zebrafish embryo. The toxic effect of $SOD1^{MT}$ on axonal outgrowth was specific and dose-dependent. No effect of $SOD1^{WT}$ was seen, indicating the selectivity of the effect for the mutant form of the protein. This $SOD1^{MT}$ axonopathy appeared motor-specific, as no toxic effect of $SOD1^{MT}$ on several other examined axonal projections was observed. In addition, the disease phenotype was independent of the type of mutation and easy to score quantitatively and in sufficient numbers to allow high-powered statistics.

It may seem paradoxical to observe a mutant SOD1-induced embryonic axonopathy, whereas ALS is an adult-onset disease. However, already very early in life, motor axonal dysfunction is also obvious in the $SOD1^{MT}$ mouse, in which clinical abnormalities only become apparent in adult life. Indeed, abnormalities of axonal transport have been described in motor neurons cultured from $SOD1^{G93A}$ mouse embryos on day 13.5 of gestation (22). Furthermore, motor neurons cultured from the same age embryos were reported to show enhanced oxyradical production, lipid peroxidation, increased intracellular calcium levels, decreased intramitochondrial

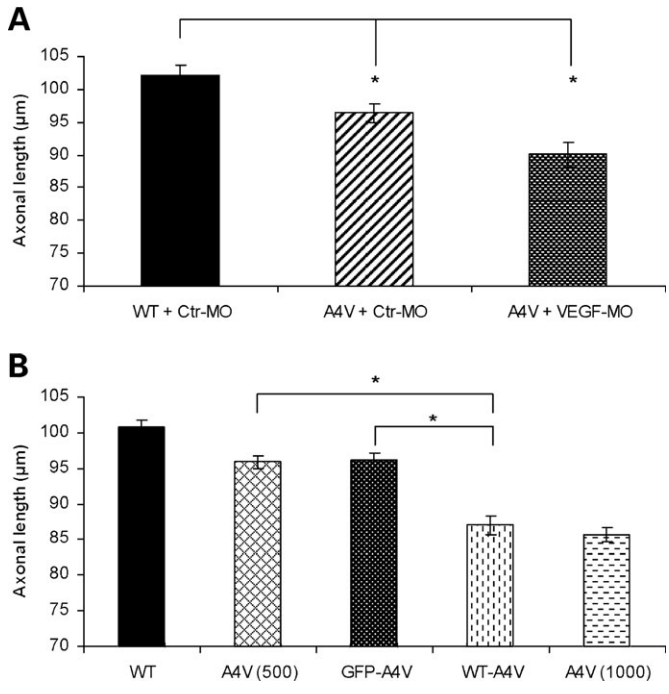

Figure 4. Lowering VEGF and co-expression of $SOD1^{WT}$ aggravate the motor neuron phenotype. Lowering VEGF by using 3 ng VEGF-MO aggravates the motor neuron phenotype induced by $SOD1^{A4V}$ 500 ng/µl ($n = 36$), compared with 3 ng Ctr-MO co-injected embryos ($n = 35$). $SOD1^{WT}$ was injected at the same concentration: 500 ng/µl ($n = 32$) (**A**). When $SOD1^{WT}$ and $SOD1^{A4V}$ are co-expressed, both 500 ng/µl ($n = 50$), a more severe phenotype is induced when compared with $SOD1^{A4V}$ 500 ng/µl ($n = 110$) or co-expression of GFP and $SOD1^{A4V}$, both 500 ng/µl ($n = 58$), equal to $SOD1^{A4V}$ 1000 ng/µl ($n = 90$), whereas $SOD1^{WT}$ 1000 ng/µl ($n = 51$) is used as a negative control (**B**). *Y*-error bars represent standard error of the mean. $^*P < 0.001$.

calcium levels and mitochondrial dysfunction (23). Increased vulnerability to excitotoxicity (24) and to a Fas-dependent pathway (25) has been described as well.

The embryonic nature of this model for a neurodegenerative disease has several major advantages. MO-based screening can identify pathogenic pathways, which can lead to new therapeutic targets for pharmacological intervention. Treatment of embryos with small compound libraries is more feasible when compared with ALS rodent models and possibly has more potential than *in vitro* models currently used for chemical screening (7). Drug testing can be performed within 2 days making high throughput screening of compounds, a promising approach to identify molecules with potential value.

Over the last years, the role of VEGF has been implicated in motor neuron disease and ALS in particular (14–17). We therefore investigated whether expression of VEGF could influence the described axonopathy. Lowering VEGF using MO knockdown technique aggravated the axonal abnormalities consistent with observations in $SOD1^{G93A}$ transgenic mice when crossed with mice expressing reduced levels of VEGF, $vegfa^{\delta/\delta}$ mice, which shortened their survival (15). Additionally, using GS4012, a compound that upregulates VEGF, the mutant SOD1-induced phenotype could be rescued almost completely. These findings emphasize the potential of VEGF in treating SOD1-induced motor neuron degeneration and hopefully for ALS in general.

Because we identified a motor neuron-specific phenotype and demonstrated two factors known to modify the phenotype of $SOD1^{MT}$-associated motor neuron degeneration in rodent models, VEGF and $SOD1^{WT}$ (14,15,17,18), to be able to influence this phenotype mimicking observations in these animals, we suggest the zebrafish to be a suitable model for studies aiming to identify disease-modifying genes and pathways contributing to pathogenesis of ALS and to screen potential therapeutic compounds. This model also is the first to concentrate on axonal abnormalities, rather than on the diseased perikaryon. Since recently it has been demonstrated that the axonopathy is an important feature in the pathogenesis of ALS (6,11), chemical and genetic screens in this model can therefore be of particular interest.

To the best of our knowledge, this is the first model for a neurodegenerative disease in the zebrafish mediated through a toxic gain of function of a mutated protein, resulting in a neuronal phenotype. MO-based knockdown of smn has yielded interesting models for the study of spinomuscular atrophy, a disease dependent on the loss of function of the survival of motor neurons (SMN) protein (10). Using the same MO technique, knockdown of spastin in the zebrafish has been described as a model for hereditary spastic paraplegia. Reduced spastin function caused defects in motor axon outgrowth, but also induced widespread defects in neuronal connectivity and extensive central nervous system-specific apoptosis, resulting in abnormal body morphology (26). Huntington's disease has been modeled in the zebrafish embryo using expression of polyQ-proteins, which resulted in insoluble inclusions. However, the phenotypes observed were developmental delay and gross abnormalities in body plan and differentiation (27) and an increase in the frequency of embryos with abnormal morphology and the occurrence of apoptosis (28), rather than a phenotype based on the loss of striatal neurons. The vertebrate model for ALS presented here is based on a phenotype specific for motor neurons. Large-scale screens using the zebrafish may assist in elucidating the pathogenesis of motor neuron degeneration and contribute to the discovery of a therapy for this dreadful disease.

MATERIALS AND METHODS

Constructs, RNA production, MO, chemicals and quantitative PCR

Human cDNA of wild-type (WT), G93A, G37R and A4V in the pCLneo vector were kind gifts from R.H. Brown Jr (Harvard Medical School, Harvard, USA). SOD1 was cloned in the pBCM vector behind a T3 promoter. The construct was linearized using Asp718. By using the mMESSAGE mMACHINE® T3 Kit (Ambion, Huntingdon, UK), RNA was transcribed from DNA and purified using the MEGAclear™ Kit (Ambion). RNA-concentration was determined using Ribogreen (Invitrogen, Carlsbad, CA, USA). The VEGF-MO published by Nasevicius *et al*. (19) (VEGF-A-3: TAAGAAAGCGAAGCTGCTGGGTATG) was a kind gift from the Flanders Institute for Biotechnology (VIB) and the Désiré Collen Research Foundation (Leuven, Belgium). As a

Table 4. Co-expression of $SOD1^{WT}$ with $SOD1^{A4V}$ results in a deterioration of branching in zebrafish embryos

	Affected embryos (%)	Odds ratio (CI)	*P*-value	Branching axons per embryo (%)
WT 1000 ng/μl, $n = 51$	19.6			4.6
A4V 500 ng/μl, $n = 110$	43.6			7.9
A4V 500 ng/μl + GFP 500 ng/μl, $n = 58$	39.7			6.6
A4V 500 ng/μl + WT 500 ng/μl, $n = 50$	74.0	3.7 (1.8–7.6)	0.00036	12.9[a,b]
A4V 1000 ng/μl, $n = 90$	71.1			11.9

Co-injection of $SOD1^{WT}$ and $SOD1^{A4V}$ induced abnormal branching in significantly more embryos when compared with $SOD1^{A4V}$-injected embryos.
[a]$SOD1^{A4V}$ (500 ng/μl) versus $SOD1^{WT}$ (500 ng/μl) + $SOD1^{A4V}$ (500 ng/μl), $P = 8.3 \times 10^{-5}$.
[b]GFP (500 ng/μl) + $SOD1^{A4V}$ (500 ng/μl) versus $SOD1^{WT}$ (500 ng/μl) + $SOD1^{A4V}$ (500 ng/μl), $P = 2.0 \times 10^{-5}$.

control MO (Ctr-MO), we used the standard control MO (CCTCTTACCTCAGTTACAATTTATA) by Gene tools (Philomath, OR, USA). For the VEGF-inducer experiment, zebrafish embryos at 6 hpf were divided in two groups and placed in GS4012 (Calbiochem, Darmstadt, Germany) dissolved in dimethyl sulfoxide (DMSO) 0.001% at a concentration of 1 ng/μl and DMSO 0.001% as a control, respectively.

Quantitative PCR was performed, as described previously (8). Total RNA was extracted from eight groups of embryos (four treated with GS4012 and four treated with 0.001% DMSO), 60 embryos per group, using the TRIPURE method followed by RNA quantification and reverse-transcribed using random hexamer priming and mMLV. Expression was quantified at 30 hpf and VEGF levels were normalized in relation to 18S expression. cDNA was quantified using the Applied Biosystems Sequence Detection System 7300. Primer and probe sequences for zebrafish *VEGF* were 5′-TGCTCCTGCAAATTCACACAA-3′, 5′-ATCTTGGCTTTTCACATCTGCAA-3′ and probe 5′-6FAM-TGCAATGCAAGTCCAGACA-MGBNFQ-3.

Zebrafish maintenance and injection

Adult zebrafish (AB strain) and embryos were maintained and staged under standard laboratory conditions (29). All experiments performed were approved by the Ethics Committee of the K.U. Leuven. Different mRNA concentrations were injected using FemtoJet (Eppendorf, Hamburg, Germany). Each injection was made in the 2–4 cell stage of the zebrafish embryo and delivered 1.76 nl mRNA or mRNA/MO solution. The volume of the droplet was determined by measuring the diameter of the droplet using a micrometer, with a droplet of mineral oil on top. The injection pressure, never exceeding 4.5 psi, was altered until the diameter of the droplet was 150 μm.

Analysis of motor neuron outgrowth and immunohistochemistry

At 30 hpf, only morphologically normal zebrafish embryos were fixed in 4% paraformaldehyde in phosphate-buffered saline (PBS) and immunostained using mouse anti-SV2 (1/200; Developmental Studies Hybridoma Bank, University of Iowa, Iowa City, IO, USA) and secondary Alexa Fluor 555 anti-mouse antibody (1/500; Molecular Probes, Eugene, OR, USA) in order to visualize motor neurons (30). Observers were blinded for injection and treatment conditions. We examined axonal defects in a total of 20 ventral motor nerves, 10 on each site along the yolk sac extension at 30 hpf. Motor neurons were scored as affected when axons branched at or above the ventral edge of the notochord (Fig. 1A). We observed branching ventral to the notochord to occur frequently in normal embryos and therefore did not take this into account. Embryos were scored abnormal when two or more axons per embryo showed aberrant branching. Axonal length was used as the second parameter in determining axonal defects. We measured the length of the first five (or 10 when indicated in the text) motor axons along the yolk sac extension from the exit point of the axon at the ventral part of the spinal cord until its distal tip using Luica software (version 4.60).

Analysis of other neuronal and non-neuronal tissues was performed after immunohistochemical staining using mouse anti-acetylated tubulin (1/200; Sigma-Aldrich, CA, USA) and mouse 3A10 (1/200; Developmental Studies Hybridoma Bank) and secondary antibody, as described earlier.

Western blot

Zebrafish embryos were dechorionated and deyolked at 30 hpf and homogenized in Radio Lummuno Precipitation Assay (RIPA) buffer containing 150 mM NaCl pH 7.5, 1% NP-40, 0.5% Na-deoxycholate, 0.1% sodium dodecyl sulfate and one tablet Complete-EDTA (Roche, Mannheim, Germany). Protein concentration was determined using the micro-BCA protein assay reaction kit 207 (Pierce, Rockford, IL, USA). Equal amounts of protein were loaded on the same blot. Western blotting was performed, as described previously (31). Primary antibodies used were rabbit polyclonal SOD1 antibody recognizing both the zebrafish and human SOD1 protein (1/10,000; SOD-100 Stressgen, Victoria, Canada) and mouse monoclonal β-actin antibody (1/5000; Sigma-Aldrich). The blots were incubated with either secondary anti-rabbit or anti-mouse alkaline phosphatase-coupled antibody (1/5000; Sigma-Aldrich). The protein bands were visualized by chemifluorescence using the enhanced chemical fluorescence (ECF) substrate (Amersham Biosciences, Buckinghamshire, UK) and scanned on a STORM 840 scanner (Molecular Dynamics, CA, USA).

Statistical analysis

Statistics were performed using SPSS 10. Experiments were analyzed with the Mann–Whitney *U*-test or the Kruskal–Wallis test, or analysis of variance. In the case of multiple

comparisons, a Bonferroni correction was performed. Bivariate correlations and tests for dose trends were analyzed using the Spearman's rank test or the Pearson's correlation coefficient, depending on the distribution of the data; χ^2 tests were used for frequency comparisons. All *P*-values reported are two-tailed and the significance level was set at 0.05.

SUPPLEMENTARY MATERIAL

Supplementary Material is available at HMG Online.

ACKNOWLEDGEMENTS

This work is supported by a grant from the Packard Center for ALS Research (Johns Hopkins University) from the University of Leuven, the Belgian Government (Interuniversity Attraction Poles, program P6/43 of the Belgian Federal Science Policy Office) and from Rotary Harelbeke. W.R. is supported through the E. von Behring Chair for Neuromuscular and Neurodegenerative Disorders.

Conflict of Interest statement. None declared.

REFERENCES

1. Walker, F.O. (2007) Huntington's disease. *Lancet*, **369**, 218–228.
2. Rosen, D.R., Siddique, T., Patterson, D., Figlewicz, D.A., Sapp, P., Hentati, A., Donaldson, D., Goto, J., O'Regan, J.P., Deng, H.X. *et al.* (1993) Mutations in Cu/Zn superoxide dismutase gene are associated with familial amyotrophic lateral sclerosis. *Nature*, **362**, 59–62.
3. Regal, L., Vanopdenbosch, L., Tilkin, P., Van Den Bosch, L., Thijs, V., Sciot, R. and Robberecht, W. (2006) The G93C mutation in superoxide dismutase 1: clinicopathologic phenotype and prognosis. *Arch. Neurol.*, **63**, 262–267.
4. Mockett, R.J., Radyuk, S.N., Benes, J.J., Orr, W.C. and Sohal, R.S. (2003) Phenotypic effects of familial amyotrophic lateral sclerosis mutant Sod alleles in transgenic *Drosophila*. *Proc. Natl. Acad. Sci. USA*, **100**, 301–306.
5. Oeda, T., Shimohama, S., Kitagawa, N., Kohno, R., Imura, T., Shibasaki, H. and Ishii, N. (2001) Oxidative stress causes abnormal accumulation of familial amyotrophic lateral sclerosis-related mutant SOD1 in transgenic *Caenorhabditis elegans*. *Hum. Mol. Genet.*, **10**, 2013–2023.
6. Gould, T.W., Buss, R.R., Vinsant, S., Prevette, D., Sun, W., Knudson, C.M., Milligan, C.E. and Oppenheim, R.W. (2006) Complete dissociation of motor neuron death from motor dysfunction by Bax deletion in a mouse model of ALS. *J. Neurosci.*, **26**, 8774–8786.
7. Zon, L.I. and Peterson, R.T. (2005) *In vivo* drug discovery in the zebrafish. *Nat. Rev. Drug Discov.*, **4**, 35–44.
8. Peterson, R.T., Shaw, S.Y., Peterson, T.A., Milan, D.J., Zhong, T.P., Schreiber, S.L., MacRae, C.A. and Fishman, M.C. (2004) Chemical suppression of a genetic mutation in a zebrafish model of aortic coarctation. *Nat. Biotechnol.*, **22**, 595–599.
9. Beattie, C.E. (2000) Control of motor axon guidance in the zebrafish embryo. *Brain Res. Bull.*, **53**, 489–500.
10. Carrel, T.L., McWhorter, M.L., Workman, E., Zhang, H., Wolstencroft, E.C., Lorson, C., Bassell, G.J., Burghes, A.H. and Beattie, C.E. (2006) Survival motor neuron function in motor axons is independent of functions required for small nuclear ribonucleoprotein biogenesis. *J. Neurosci.*, **26**, 11014–11022.
11. Fischer, L.R., Culver, D.G., Tennant, P., Davis, A.A., Wang, M., Castellano-Sanchez, A., Khan, J., Polak, M.A. and Glass, J.D. (2004) Amyotrophic lateral sclerosis is a distal axonopathy: evidence in mice and man. *Exp. Neurol.*, **185**, 232–240.
12. Amendola, J., Verrier, B., Roubertoux, P. and Durand, J. (2004) Altered sensorimotor development in a transgenic mouse model of amyotrophic lateral sclerosis. *Eur. J. Neurosci.*, **20**, 2822–2826.
13. Lindberg, M.J., Bystrom, R., Boknas, N., Andersen, P.M. and Oliveberg, M. (2005) Systematically perturbed folding patterns of amyotrophic lateral sclerosis (ALS)-associated SOD1 mutants. *Proc. Natl. Acad. Sci. USA*, **102**, 9754–9759.
14. Azzouz, M., Ralph, G.S., Storkebaum, E., Walmsley, L.E., Mitrophanous, K.A., Kingsman, S.M., Carmeliet, P. and Mazarakis, N.D. (2004) VEGF delivery with retrogradely transported lentivector prolongs survival in a mouse ALS model. *Nature*, **429**, 413–417.
15. Lambrechts, D., Storkebaum, E., Morimoto, M., Del-Favero, J., Desmet, F., Marklund, S.L., Wyns, S., Thijs, V., Andersson, J., van Marion, I. *et al.* (2003) VEGF is a modifier of amyotrophic lateral sclerosis in mice and humans and protects motoneurons against ischemic death. *Nat. Genet.*, **34**, 383–394.
16. Oosthuyse, B., Moons, L., Storkebaum, E., Beck, H., Nuyens, D., Brusselmans, K., Van Dorpe, J., Hellings, P., Gorselink, M., Heymans, S. *et al.* (2001) Deletion of the hypoxia-response element in the vascular endothelial growth factor promoter causes motor neuron degeneration. *Nat. Genet.*, **28**, 131–138.
17. Storkebaum, E., Lambrechts, D., Dewerchin, M., Moreno-Murciano, M.P., Appelmans, S., Oh, H., Van Damme, P., Rutten, B., Man, W.Y., De Mol, M. *et al.* (2005) Treatment of motoneuron degeneration by intracerebroventricular delivery of VEGF in a rat model of ALS. *Nat. Neurosci.*, **8**, 85–92.
18. Deng, H.X., Shi, Y., Furukawa, Y., Zhai, H., Fu, R., Liu, E., Gorrie, G.H., Khan, M.S., Hung, W.Y., Bigio, E.H. *et al.* (2006) Conversion to the amyotrophic lateral sclerosis phenotype is associated with intermolecular linked insoluble aggregates of SOD1 in mitochondria. *Proc. Natl. Acad. Sci. USA*, **103**, 7142–7147.
19. Nasevicius, A., Larson, J. and Ekker, S.C. (2000) Distinct requirements for zebrafish angiogenesis revealed by a VEGF-A morphant. *Yeast*, **17**, 294–301.
20. Stalmans, I., Lambrechts, D., De Smet, F., Jansen, S., Wang, J., Maity, S., Kneer, P., von der Ohe, M., Swillen, A., Maes, C. *et al.* (2003) VEGF: a modifier of the del22q11 (DiGeorge) syndrome? *Nat. Med.*, **9**, 173–182.
21. Bruijn, L.I., Houseweart, M.K., Kato, S., Anderson, K.L., Anderson, S.D., Ohama, E., Reaume, A.G., Scott, R.W. and Cleveland, D.W. (1998) Aggregation and motor neuron toxicity of an ALS-linked SOD1 mutant independent from wild-type SOD1. *Science*, **281**, 1851–1854.
22. Kieran, D., Hafezparast, M., Bohnert, S., Dick, J.R., Martin, J., Schiavo, G., Fisher, E.M. and Greensmith, L. (2005) A mutation in dynein rescues axonal transport defects and extends the life span of ALS mice. *J. Cell. Biol.*, **169**, 561–567.
23. Kruman, I.I., Pedersen, W.A., Springer, J.E. and Mattson, M.P. (1999) ALS-linked Cu/Zn-SOD mutation increases vulnerability of motor neurons to excitotoxicity by a mechanism involving increased oxidative stress and perturbed calcium homeostasis. *Exp. Neurol.*, **160**, 28–39.
24. Van Damme, P., Dewil, M., Robberecht, W. and Van Den Bosch, L. (2005) Excitotoxicity and amyotrophic lateral sclerosis. *Neurodegener. Dis.*, **2**, 147–159.
25. Raoul, C., Estevez, A.G., Nishimune, H., Cleveland, D.W., deLapeyriere, O., Henderson, C.E., Haase, G. and Pettmann, B. (2002) Motoneuron death triggered by a specific pathway downstream of Fas. potentiation by ALS-linked SOD1 mutations. *Neuron*, **35**, 1067–1083.
26. Wood, J.D., Landers, J.A., Bingley, M., McDermott, C.J., Thomas-McArthur, V., Gleadall, L.J., Shaw, P.J. and Cunliffe, V.T. (2006) The microtubule-severing protein Spastin is essential for axon outgrowth in the zebrafish embryo. *Hum. Mol. Genet.*, **15**, 2763–2771.
27. Miller, V.M., Nelson, R.F., Gouvion, C.M., Williams, A., Rodriguez-Lebron, E., Harper, S.Q., Davidson, B.L., Rebagliati, M.R. and Paulson, H.L. (2005) CHIP suppresses polyglutamine aggregation and toxicity *in vitro* and *in vivo*. *J. Neurosci.*, **25**, 9152–9161.
28. Schiffer, N.W., Broadley, S.A., Hirschberger, T., Tavan, P., Kretzschmar, H.A., Giese, A., Haass, C., Hartl, F.U. and Schmid, B. (2007) Identification of anti-prion compounds as efficient inhibitors of polyglutamine protein aggregation in a zebrafish model. *J. Biol. Chem.*, **282**, 9195–9203.
29. Westerfield, M. (2003) *The Zebrafish Book*. The University of Oregon Press, Eugene, Oregon.
30. Panzer, J.A., Gibbs, S.M., Dosch, R., Wagner, D., Mullins, M.C., Granato, M. and Balice-Gordon, R.J. (2005) Neuromuscular synaptogenesis in wild-type and mutant zebrafish. *Dev. Biol.*, **285**, 340–357.
31. Krishnan, J., Lemmens, R., Robberecht, W. and Van Den Bosch, L. (2006) Role of heat shock response and Hsp27 in mutant SOD1-dependent cell death. *Exp. Neurol.*, **200**, 301–310.